Journal of Environmental Management 324 (2022) 116363

Contents lists available at ScienceDirect

Journal of Environmental Management

journal homepage: www.elsevier.com/locate/jenvman

Research article

Biofilm-based simultaneous nitrification, denitrification, and phosphorous uptake in wastewater by *Neurospora discreta*

Shamas Tabraiz [a], N.M. Aiswarya [b], Himani Taneja [a], R. Aravinda Narayanan [b], Asma Ahmed [a,*]

[a] Section of Natural and Applied Sciences, Canterbury Christ Church University, UK
[b] Department of Physics, Birla Institute of Technology and Science Pilani, Hyderabad Campus, India

ARTICLE INFO

Keywords:
Fungal biofilms
Simultaneous nitrification and denitrification
Phosphorous removal
Wastewater treatment

ABSTRACT

Biological removal of nitrogen and phosphorous from wastewater conventionally involves multiple processing steps to satisfy the differing oxygen requirements of the microbial species involved. In this work, simultaneous nitrification, denitrification, and phosphorous removal from synthetic wastewater were achieved by the fungus *Neurospora discreta* in a single-step, biofilm-based, aerobic process. The concentrations of carbon, nitrogen, and phosphorous in the synthetic wastewater were systematically varied to investigate their effects on nutrient removal rates and biofilm properties. Biofilm growth was significantly ($p < 0.05$) affected by carbon and nitrogen, but not by phosphorous concentration. Scanning electron microscopy revealed the effects of nutrients on biofilm microstructure, which in turn correlated with nutrient removal efficiencies. The carbohydrate and protein content in the biofilm matrix decreased with increasing carbon and nitrogen concentrations but increased with increasing phosphorous concentration in the wastewater. High removal efficiencies of carbon (96%), ammonium (86%), nitrate (100%), and phosphorus (82%) were achieved under varying nutrient conditions. Interestingly, decreasing the phosphorus concentration increased the nitrification and denitrification rates, and decreasing the nitrogen concentration increased the phosphorus removal rates significantly ($p < 0.05$). Correlations between biofilm properties and nutrient removal rates were also evaluated in this study.

1. Introduction

Increasing industrialization and inadequate treatment of industrial wastewaters have led to large amounts of nitrogen and phosphorus compounds being discharged into water bodies (Sinha et al., 2017; Wurtsbaugh et al., 2019). High concentrations of nitrogen and phosphorus in the influent wastewater cause eutrophication involving the excessive growth of algae and cyanobacteria in water bodies, and lead to the deterioration of water quality to a level that is harmful to humans and aquatic life (Tang et al., 2019; Zhang et al., 2020). Nitrogen and phosphorus removal from the wastewater is therefore critical for safe disposal to avoid eutrophication in surface waters.

Currently, phosphorus is removed from wastewaters either chemically, by precipitation, or biologically, using microorganisms. Enhanced biological phosphorus removal processes using polyphosphate-accumulating organisms (PAO) for phosphorus removal provide a cost-effective, environmentally friendly opportunity to recover the phosphorus from biomass (Ge et al., 2015; Rashid et al., 2020). However, PAOs require both anaerobic and aerobic conditions to accumulate phosphorus. Under anaerobic conditions, PAOs use polyphosphate (poly-P) and glycogen as energy sources, take up carbon and volatile fatty acids and store them as polyhydroxyalkanoates (PHA). Stored PHAs are used as an energy source to replenish the glycogen and store the poly-P under aerobic conditions (Nielsen et al., 2019). Therefore, sludge must be circulated in separate reactors of the wastewater treatment plant to create the aerobic and anaerobic cycles, rendering the process complicated and expensive (Rey-Martínez et al., 2019; Zhao et al., 2021). A few fungal strains have been recently reported as potential replacements for bacterial PAOs (He et al., 2019; Zeng et al., 2021), but further research is needed in this area.

Nitrogen removal from wastewater requires physicochemical processes along with biological treatment. Biological nutrient removal (BNR) predominantly involves bacterial nitrification and denitrification processes using sequential anaerobic-anoxic-oxic batch reactors (Pathak, 2020; Vogel, 1956; Tabraiz et al., 2018; Winkler and Straka, 2019). The nitrification process is carried out in two steps: initially,

* Corresponding author. Section of Natural and Applied Sciences, School of Psychology and Life Sciences, Canterbury Christ Church University, North Holmes Road, Canterbury, CT1 1QU, United Kingdom.
E-mail address: asma.ahmed@canterbury.ac.uk (A. Ahmed).

https://doi.org/10.1016/j.jenvman.2022.116363
Received 5 July 2022; Received in revised form 14 September 2022; Accepted 22 September 2022
Available online 5 October 2022

ammonia is oxidized into nitrite by ammonia-oxidizing bacteria (AOB) then nitrite is oxidized to nitrate by nitrite-oxidizing bacteria (NOB) under aerobic conditions. Heterotrophic denitrifying bacteria convert nitrate to gaseous forms of nitrogen (N_2, N_2O) under anoxic conditions and require carbon as an electron donor (Ren et al., 2020). AOB and NOB are slow-growing microorganisms that are sensitive to environmental conditions, while denitrifying bacteria typically grow only in anoxic conditions (Huang et al., 2017; Sun et al., 2016). Therefore, most of the BNR technologies require at least two sequential reactors to create a suitable environment for AOB, NOB and denitrifying bacteria. Such processes suffer from low nitrification rates and the need for strict control of culture conditions, and require relatively long processing times to achieve high removal efficiencies, which make them expensive to run (Ji et al., 2020).

Recently, a few microorganisms called heterotrophic nitrifying and aerobic denitrifying microorganisms (HNADMs) have been reported, which can oxidize ammonia and perform denitrification in a single aerobic reactor (Song et al., 2021; Wang and He, 2020). In such processes, inorganic nitrogen is converted into organic nitrogen (biomass) and gaseous nitrogen by HNADMs. Bacterial HNADMs catalyse ammonia into hydroxylamine using ammonia monooxygenase enzymes, followed by its conversion to nitrite by hydroxylamine oxidoreductase enzymes or pyruvic oxime dioxygenase. Nitrite is then converted to nitrate using nitrite oxidoreductase. In the denitrification step, nitrate is converted into nitrite by using nitrite oxidoreductases followed by nitrite reduction to nitric oxide by a copper-containing nitrite reductase, then to nitrous oxide using nitric oxide reductase, and finally to nitrogen (N_2) gas using nitrous oxide reductase (Song et al., 2021). Bacterial HNADM strains isolated from various environments belong to the *Pseudomonas*, *Acinetobacter*, *Cuprobacter*, *Bacillus*, *Cupriavidus*, *Halmonas*, *Klebsiella*, *Marinobacter* and *Photobacterium* genera (Huang et al., 2020; Sun et al., 2016). Although fungi are known to have several advantages over bacteria in wastewater treatment processes, including the ability to degrade complex pollutants and the ability to withstand fluctuations in the environment, research on fungal HNADMs has been limited. Only a few fungal strains (*Penicillium tropicum*, *Henseniaspor uvarum, Fusarium solani*) have been reported for their heterotrophic nitrification and aerobic denitrification ability (Cheng et al., 2020; Zhang et al., 2018). Furthermore, there is limited understanding of the effects of the carbon, nitrogen, and phosphorus concentrations in wastewater on denitrification and nitrification rates.

The present study evaluates the biofilms of a novel fungus *Neurospora discreta* for simultaneous removal of carbon, nitrogen and phosphorous in synthetic wastewater. This fungus was chosen for its ability to withstand a wide range of growth conditions (Romero-Olivares et al., 2015), degrade complex contaminants (Pamidipati and Ahmed, 2017), grow on multiple substrates, and form strong biofilms on the air-liquid interface (Ahmed et al., 2020). This unique combination of characteristics makes *N. discreta* a promising candidate for wastewater treatment. Biofilm-based reactors are known to be more efficient compared to conventional mixed-culture reactors in wastewater treatment, owing to the higher cell densities and higher tolerance of biofilms towards contaminants (Van Acker 2014). The use of *N. discreta* biofilms offers the following additional advantages overall conventional wastewater treatment processes: (1) the formation of strong biofilms on the air-liquid interface eliminates the need for additional support materials or specific reactor systems for biofilm growth. (2) These biofilms facilitate easy separation of cells from the treated water, thereby minimising the need for a secondary clarifier, which is an essential unit in most conventional wastewater treatment processes. (3) Simultaneous nitrification and denitrification under aerobic conditions in a single reactor can reduce the operational and handling complexities of the existing biological processes for nitrification and denitrification.

This work is based on the hypothesis that the concentrations of nutrients in the wastewater influence nutrient removal efficiencies as well as the properties of the biofilms formed during the process. Therefore, this study investigates the effects of nutrient concentrations on the nitrification, denitrification, phosphorus, and carbon removal efficiencies by *N. discreta* biofilms, as well as on biofilm properties including growth, extracellular polymeric substances (EPS) composition, and water retention value (WRV). As the properties of biofilms play an important role in the interaction between the wastewater and the cells, this study also evaluates the correlations between biofilm properties and nutrient removal rates.

2. Materials and methods

2.1. Inoculum preparation

A fungal strain *Neurospora discreta*, isolated from a Subabul tree (*Leucaena leucocephala*), and identified and reported in our previous study (Pamidipati and Ahmed, 2017) was used for the present work. The phylogenetic tree constructed from the 18S rRNA internal transcribed spacer (ITS) gene sequence obtained from the CSIR-Institute of Microbial Technology, Chandigarh, India is provided in the supplementary material (Figure S1).

The inoculum for the present study was prepared by growing *N. discreta* on potato dextrose agar (PDA) plates at 30 $^{\circ}C$ for 3 days, and gently scraping the cells from the PDA plates and suspending in synthetic wastewater (30 mL) without KH_2PO_4, NH_4NO_3, or sucrose. The spore and filament suspension of fungus was centrifuged at 5000$\times g$ for 5 min. The supernatant was discarded, and the pellet was resuspended in the synthetic wastewater again. The solution was filtered through a sterile muslin cloth to remove the filaments from solution. A solution of 1×10^7 spores per mL was prepared and 1 mL of it was used to inoculate each batch reactor.

2.2. Wastewater composition and reactor set-up

Synthetic wastewater was prepared based on a modified recipe of Vogel's media (Pamidipati and Ahmed, 2017) by dissolving the following chemicals in deionized water; Na_3 citrate.$2H_2O$ (2.5 g L^{-1}), KH_2PO_4 (5.0 g L^{-1}), NH_4NO_3 (2.0 g L^{-1}), $MgSO_4.7H_2O$ (0.2 g L^{-1}), $CaCl_2.2H_2O$ (0.1 g L^{-1}), sucrose (20 g L^{-1}) and trace element solution (0.1 mL.L^{-1}). The trace element solution was prepared by dissolving the following chemicals in deionized water: citric acid monohydrate (50 g L^{-1}), $ZnSO_4.7H_2O$ (50 g L^{-1}), $Fe(NH_4)_2(SO_4)_2.6H_2O$ (10 g L^{-1}), $CuSO_4.5H_2O$ (2.5 g L^{-1}), $MnSO_4.H_2O$ (0.5 g L^{-1}), H_3BO_3 (0.5 g L^{-1}) and $Na_2MoO_4.2H_2O$ (0.5 g L^{-1}).

Overall, three trials were set-up as follows (Table 1): (1) nitrogen

Table 1
Nutrient concentrations in the (N), phosphorus (P), and carbon (C) trials.

Concentration in solution (g L^{-1})			
Reactor	C	N	P
Nitrogen trial			
NA	8.41	0.70	1.13
NB	8.41	0.35	1.13
NC	8.41	0.175	1.13
ND	8.41	0.044	1.13
NE	8.41	0.011	1.13
Phosphorus trial			
PA	8.41	0.70	1.13
PB	8.41	0.70	0.564
PC	8.41	0.70	0.282
PD	8.41	0.70	0.070
PE	8.41	0.70	0.017
Carbon trial			
CA	8.41	0.70	1.13
CB	4.21	0.70	1.13
CC	2.10	0.70	1.13
CD	0.53	0.70	1.13
CE	0.13	0.70	1.13

trial, in which the concentration of NH_4NO_3 in the wastewater was varied (2) phosphorous trial, in which the concentration of KH_2PO_4 was varied and (3) carbon trial in which the concentration of sucrose was varied. In each trial the concentrations of all remaining components were constant. All experiments were performed in 250 mL Erlenmeyer flasks containing 100 mL of wastewater. Each trial consisted of five sets of reactors with varying concentrations of carbon, nitrogen, and phosphorous in triplicate. Reactors containing the wastewater were autoclaved (121 °*C*, for 15 min) and 0.1 mL sterile biotin solution (100 mg L^{-1}) was added to each reactor after cooling to room temperature. After inoculation, as described in section 2.1, the reactors were placed in an incubator at 30 °*C* without any agitation. Biofilms were harvested on the 7th day of the experiment. Biofilm samples for physico-chemical characterization were extracted immediately, and the remaining samples were stored by submerging in isopropyl alcohol (70%) for microscopy.

2.3. Biofilm growth rate, water retention value and dry weight

Water retention value (WRV) of the harvested biofilms was determined using a modified method of Tappi UM 256. Briefly, a preweighted biofilm sample was soaked in the tap water for an hour, weighed again and centrifuged at 1217×*g*. The supernatant was removed, and the biomass pellet was dried at 103.5 °*C* until constant weight was achieved. The difference between wet weight and dry weight was divided by the wet weight to get the WRV.

The normalized dry mass of the biofilm was also calculated by dividing the dry weight by the wet weight. The dry weight of the biofilm was used to calculate the biofilm biomass per unit volume of the reactor (Ahmed et al., 2020).

The specific growth rates of the biofilms were calculated using equation (1).

$$\mu = \frac{ln\,(X_1/X_0)}{(T_1 - T_0)} \tag{1}$$

Where "μ" is the specific growth rate (d^{-1}), "X_1" is the dry biomass concentration (g L^{-1}) of the biofilm on day "T_1" and "X_0" is the inoculum dry biomass concentration (g L^{-1}) on day "T_0".

2.4. Extraction of extracellular polymeric substances (EPS)

A 10 mL solution of formaldehyde (0.22%) and sodium chloride (8.5%) was prepared in a 50 mL centrifuge tube. The weighted biofilm sample (wet, drained) was suspended in the solution. The biofilm suspension was placed at 4 °*C* for 3 h, after which the suspension was centrifuged at 10000×*g* for 10 min. The supernatant obtained was filtered (0.22 μm) and saved for further analysis (Ahmed et al., 2020; Liu and Fang, 2002).

2.5. Determination of carbohydrate and protein content in EPS

The dinitro salicylic acid reagent (DNS) method was used to measure the carbohydrates (Gonalves et al., 2010) as follows: the DNS reagent was prepared by dissolving 2.5 g of dinitro salicylic acid (Acros Organics) in 125 mL of deionized water at 80°*C*. The solution was cooled down at room temperature and 50 mL of sodium hydroxide (2N) was added. Potassium sodium tartrate tetra hydrate (75 g) was added to the solution and a total volume of 250 mL was achieved by adding deionized water. To hydrolyse the sample, 1 mL of sample was taken and mixed with 0.25 mL of concentrated sulfuric acid. The solution was kept in a water bath at 95 °C for 1 h. The tubes were taken out and cooled to room temperature and neutralized with 10 N sodium hydroxide. 75 μL DNS solution was mixed with 75 μL of the sample solution in 96-well plate. The 96-well plate was placed in a pre-heated oven at 100 °C for 30 min. The plate was removed and 75 μL ice cold deionized water was mixed in each well and kept refrigerated at 4 °C for 15 min. The absorbance was measured at 540 nm in spectrophotometer (MULTISKAN GO) and the carbohydrate concentration was calculated using an appropriate calibration curve.

The protein concentration in the EPS was measured using a colorimetric protein quantification kit (77371, Sigma Aldrich, UK) according to the manufacturer's protocol.

2.6. Wastewater characterization

The synthetic wastewater was characterized by measuring the carbon, nitrogen, and phosphorous concentrations, as well as pH and dissolved oxygen levels. Total organic carbon (TOC) in terms of simple sugars was determined on days 0 and 7 using the DNS method described in section 2.5. NH_4–N and PO_4–P concentrations were analysed using test kits (100683 & 100798, Merck, UK). NO_3–N and NO_2–N concentrations were measured using test kits (1176802 & 1177230, Camlab, UK). pH was monitored at the start and end of the experiment using pH meter (HQ430D, Hach). Dissolved oxygen (DO) was measured using DO meter (HI 9142, HANNA, UK).

Nutrient removal efficiencies and removal rates were calculated using the following equations:

$$Removal\ Efficiency\ R.E\ (\%) = \left(\frac{C_0 - C_t}{C_0}\right) \times 100 \tag{2}$$

$$Nutrient\ Removal\ Rate = \frac{C_0 - C_t}{T} \tag{3}$$

$$Total\ Nutrient\ Removal = M_0 - M_t \tag{4}$$

$$Specific\ Nutrient\ Removal = \frac{M_0 - M_t}{Biofilm\ dry\ biomass} \tag{5}$$

$$Specific\ Nutrient\ Removal\ Rate = \frac{M_0 - M_t}{(Biofilm\ dry\ biomass) \times T} \tag{6}$$

Where "*R.E*" is removal efficiency, "C_0" is concentration of nutrient (C, N and P) on day 0, and "C_t" is concentration of nutrient on day 7, "M_0" is the mass of nutrient on day 0, "M_t" the mass of the nutrient on day 7 and "*T*" is the duration of the experiment (7 days).

2.7. Biofilm microstructure

Microstructural characterization of biofilms was carried out using Field Emission Scanning Electron Microscopy (FESEM) Apreo S, FEI. Samples were dried for 48hrs in the desiccator before analysis. SEM investigations were performed at magnifications of 1500X, 2500X, 5000X.

Bright field images were analysed using ImageJ software (US National Institutes of Health) to measure the filament length, thickness, and area of areal pores (Huang and Wang, 1995). SEM images were analysed at 2500× magnification, at a scale of 9.27 pixels per micron (μm). The length and thickness of the filaments were measured manually using segmented line function of ImageJ (Abràmoff et al., 2004). Total area of the visible pores was measured by first converting the bright field images into 8-bit followed by applying the thresholding algorithm to get the total aerial pore area for each biofilm (Huang and Wang, 1995).

2.8. Statistical analysis

The *t*-test was applied to determine whether differences in removal efficiencies at varying nutrient concentrations are statistically significant. A heat map of Pearson's correlation between biofilm properties and nutrient removal was generated using the "CorLevelPlot" package in R Software (v4.1.2).

3. Results and discussion

3.1. Biofilm growth

Biofilm growth at the air-liquid interface of the reactors commenced within 24–36 h post-inoculation. Thereafter, the thickness of the biofilms increased with the formation of new layers. Biofilm growth was significantly affected by the carbon and nitrogen concentrations in the synthetic wastewater (Fig. 1a and c). Representative images of harvested biofilms provided in the supplementary data also indicate these differences (Figure S2). Dry biomass measured the highest at the nitrogen concentration of 0.175 g L^{-1} (C:N = 48) (Fig. 1a). Further increase in the nitrogen concentration had no effect on growth. In the case of phosphorus, the optimal dry biomass was observed at concentration of 0.56 g L^{-1} (C:P = 15). Decrease in the phosphorus concentration to 0.07 g L^{-1} (C:P = 120) had no significant ($p > 0.05$) effect on the dry biomass of the biofilm. However, further decrease to 0.017 g L^{-1} (C:P = 494) decreased the dry biomass significantly ($p < 0.05$) (Fig. 1b). Whilst in the case of carbon, increase in the concentration increased the dry biomass of biofilms, which did not plateau, indicating the ability of the fungus to consume even higher levels of carbon and C:N ratio, as well as its ability to grow on relatively low nitrogen concentrations in the synthetic wastewater (Fig. 1c). The maximum specific growth rate of 0.8 d^{-1} was observed on the optimal growth C: N of 48. Change in the nitrogen and carbon concentration also affected the specific growth rates. However, phosphorus had no significant effect on the specific growth rates (Fig. 1d).

3.2. Biofilm composition, water retention value and microstructure

Chemical analysis of the biofilms revealed that protein and polysaccharide concentrations per unit dry biomass in the EPS decreased as the concentration of nitrogen and carbon increased (Fig. 1a and c and S3). This can be attributed to the following reason: lower concentration of nitrogen and carbon led to the starvation of the cells, which resulted in higher protein concentration per unit biomass in EPS. The phenomenon of increased EPS production under conditions of starvation has been reported in other microorganisms as well (Myszka and Czaczyk, 2009; Zhang et al., 2014). When grown on sub-optimal C:N ratios, the metabolic energy seems to be diverted towards EPS production instead of biomass production. In such conditions, the EPS tends to store the nutrients available in excess (Flemming and Wingender, 2010). In the present study, under conditions of low carbon, nitrogen and phosphate were in excess whilst under low nitrogen conditions, carbon and phosphate were in excess.

In the phosphorus trial, protein and polysaccharide concentrations per unit biomass in the EPS increased as the concentration of the phosphorus increased from 0.282 to 1.13 g L^{-1} (Fig. 1b and S3). As reported by Zeng et al. fungi tend to store a large fraction of the phosphate in the EPS (Zeng et al., 2021), which explains the effects observed in the present study. A further discussion on the relationship between phosphorous uptake and biofilm properties is presented in section 3.6.

In the present study, the WRV of biofilms increased with increasing nutrient concentrations, although the influence of phosphorous on WRV was not very strong (Fig. 1a, b and 1c). WRV provides insight into the hydrophilicity and water holding capacity of a material. In case of

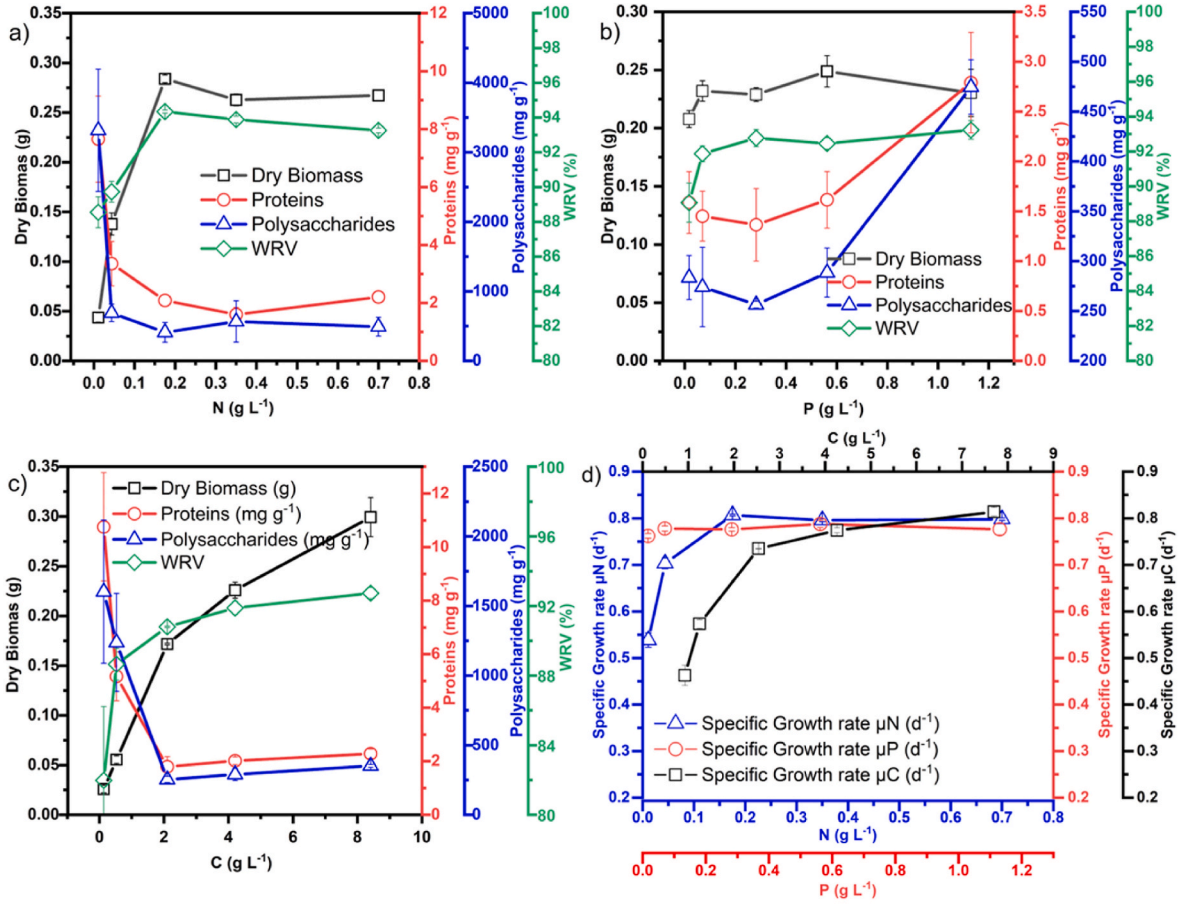

Fig. 1. Biofilm growth and properties. Dry biomass, proteins per unit biomass (mg g^{-1}), polysaccharides per unit biomass (mg g^{-1}), and water retention value (WRV) of the biofilms in (a) nitrogen, (b) phosphorus, and (c) carbon trials, harvested on the 7th day of experiment vs nutrient's concentration. Specific growth rate (μ d^{-1}) curves of nitrogen, carbon, and phosphorus are shown in (d).

biofilms, WRV is closely related to the composition and microstructure of biofilms and can affect the interaction between the cells embedded in the biofilms, and nutrients in the environment (Narayanan and Ahmed, 2019). The WRV trends showed a significant ($p < 0.05$) inverse relation with polysaccharides (mg g^{-1}) and proteins (mg g^{-1}) in the nitrogen and carbon trials as shown in the supplementary data (Figure S4). This can be attributed to increased hydrophobicity (and therefore, reduced WRV) of the EPS in low nutrient conditions due to stress, which has been reported in other fungi *Phanerochaete chrysosporium* (Cao et al., 2018). However, decreasing the phosphorous concentration did not impact the WRV significantly, just as it did not affect biofilm growth, indicating that the cells did not experience stress at the low phosphorous levels tested in this study.

SEM images of the biofilms revealed fungal hyphae (filaments) embedded in an EPS matrix with micron and nano-sized pores (Narayanan and Ahmed, 2019). As seen in Fig. 2a, b, and c, filament length showed an inverse correlation with nutrient concentrations, which can be explained by the fact that fungi are non-motile, and hence grow in length seeking nutrients (Moore et al., 2020; Narayanan and Ahmed, 2019). This can also be seen from the strong negative correlations ($p < 0.001$) in Figure S3. Similarly, filament diameter had an inverse relation with nitrogen and phosphorus concentrations. On the other hand, the area of pores increased as the nitrogen and phosphorus concentrations increased which can be attributed to the decrease in filament diameter. However, an increase in carbon concentration increased the filament diameter. The trends in pore area with varying nitrogen concentration can also be seen in the representative SEM images from the nitrogen trial in Fig. 2(d–f). The effects of nutrients on biofilm microstructure and its relation to nutrient removal efficiencies are further discussed in section 3.6.

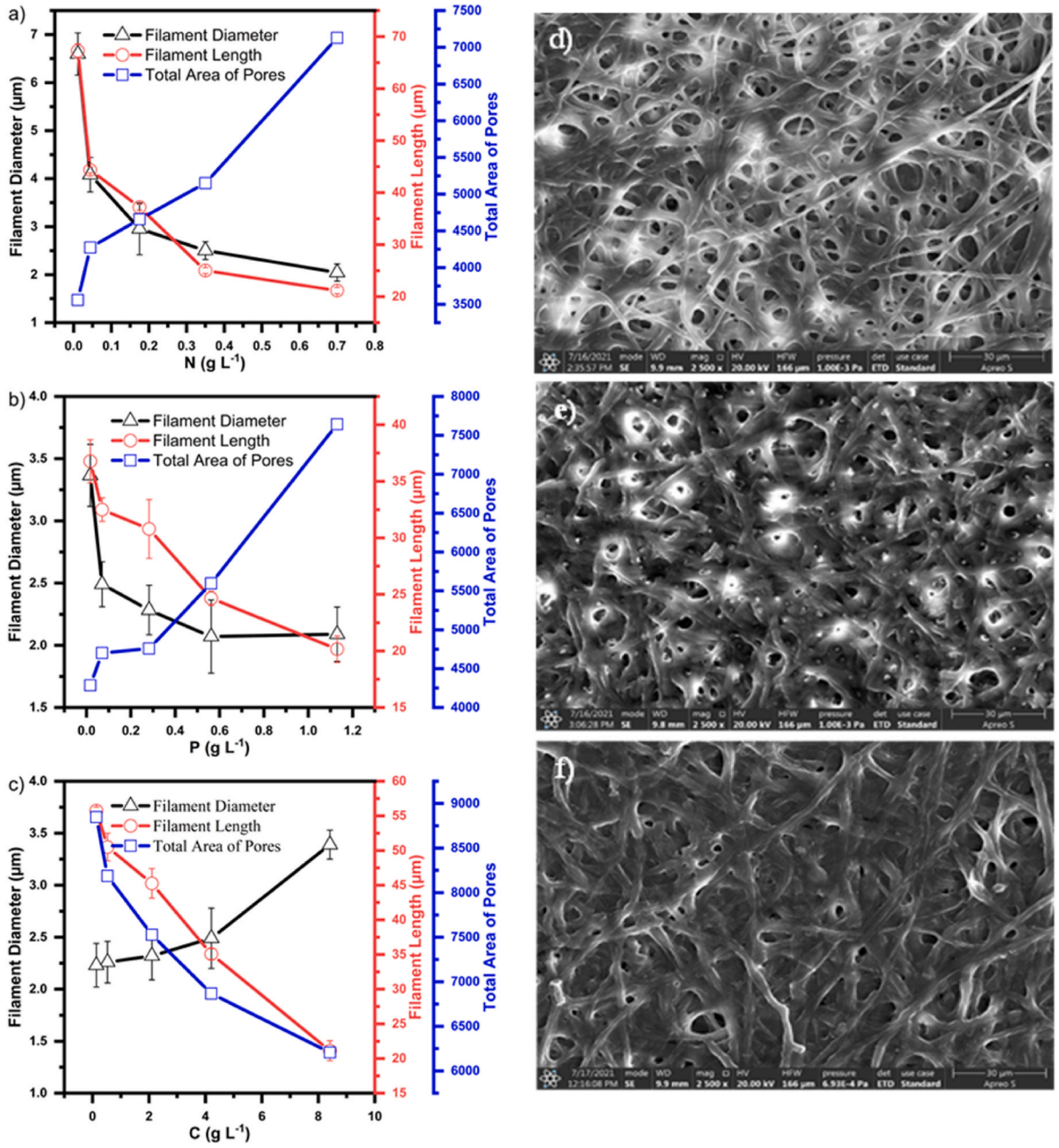

Fig. 2. Biofilm microstructure. Average filament diameter, length, and total area of pores of biofilms harvested from the a) nitrogen trial, b) phosphorus trial and c) carbon trial (error bars showing standard deviation, n = 3). SEM images of biofilms from nitrogen trial bioreactor at magnifications of 2500 × d) NA (nitrogen conc. = 0.7 g L^{-1}), e) NC (nitrogen conc. = 0.175 g L^{-1}) f) ND (nitrogen conc. = 0.044 g L^{-1}).

3.3. Carbon and phosphorus removal

The highest carbon removal efficiency was ~96.7%, demonstrating the potential application of *N. discreta* biofilms in treating wastewaters with higher organic content. Carbon removal efficiencies increased significantly ($p < 0.05$) as the nitrogen concentration increased from 0.011 to 0.175 g L^{-1} (Fig. 3a). Thereafter, an increase in the nitrogen concentration had no significant ($p > 0.05$) effect on the carbon removal. In the phosphorus trial, no significant ($p > 0.05$) change in the removal efficiency of carbon was observed as the phosphorus concentration was increased (C:P was decreased) (Fig. 3b). It can be inferred that a very low concentration of phosphorus (<0.017 g L^{-1}, C:P = 495) is required for cell growth and metabolic functioning. In the carbon trial, as the carbon concentration increased from 0.13 to 2.1 g L^{-1} (C:N ratio from 0.18 to 3), the carbon removal efficiency increased significantly ($p < 0.05$) (Fig. 3c). However, further increase in carbon and C:N did not affect carbon removal efficiency. It should be noted that at lower carbon concentrations in the carbon trials, the measured carbon could partly be due to the EPS secreted by cells or lysis of dead cells.

Phosphorus removal efficiencies were affected by nitrogen, carbon, and phosphorous concentrations (Fig. 3d, e, and f). In the nitrogen trial, higher phosphorus removal efficiencies were observed at lower nitrogen concentrations (higher C:N) (Fig. 3d), besides the lower biomass of biofilm (Fig. 1a). In the carbon trial, phosphorous removal was proportional to carbon concentration (Fig. 3f). In the phosphorus trial, phosphorous removal was highest (82%) at the lowest phosphorus concertation (0.017 g L^{-1}, C:P = 495) and significantly ($p < 0.05$) higher than the remaining concentrations. However, no clear trend was seen at higher concentrations (Fig. 3e). A recent study reported phosphorus removal (~85%) from wastewater containing 0.012 g L^{-1} phosphorus,

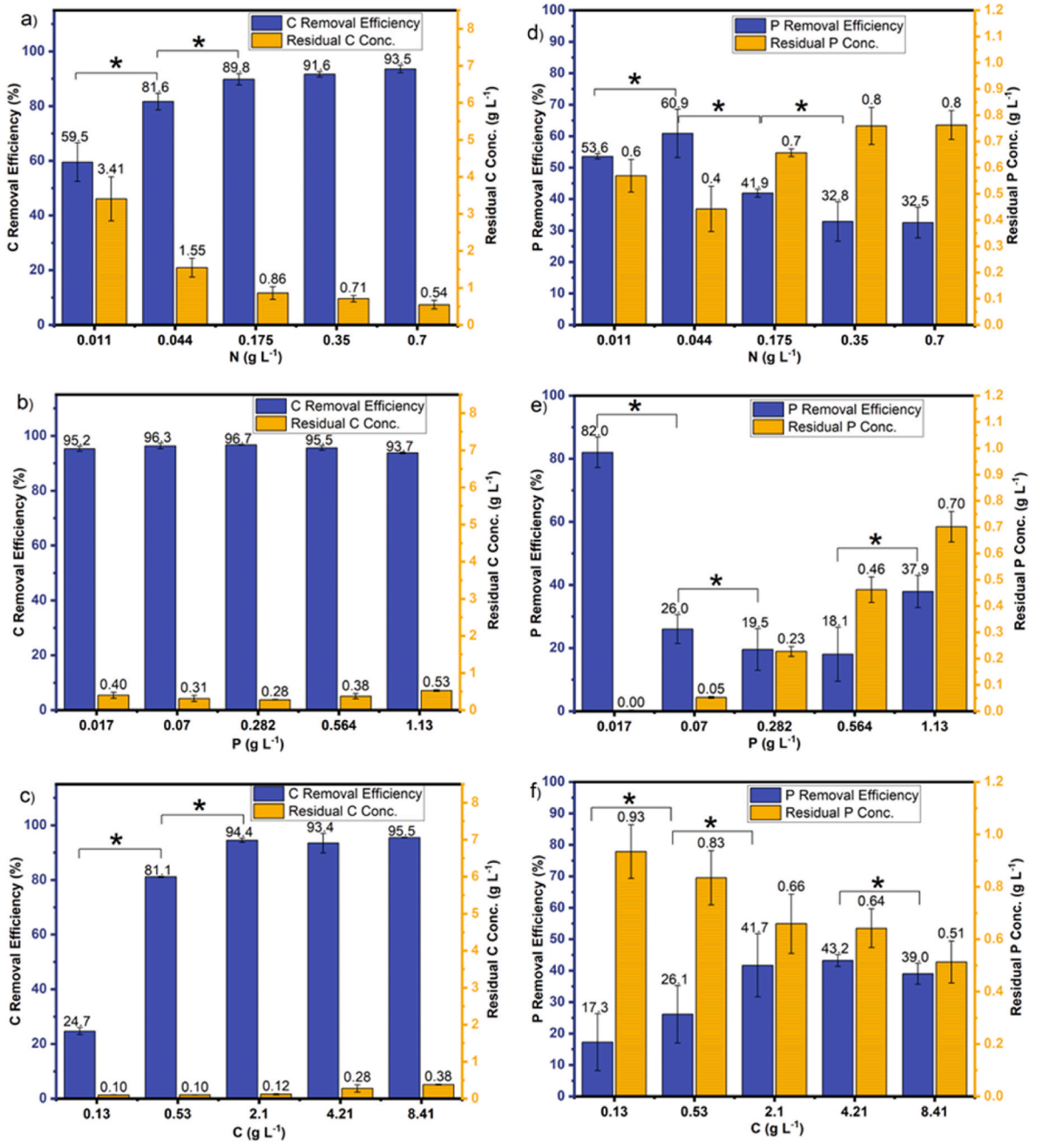

Fig. 3. Carbon (a, b & c) and phosphorus (d, e & f) removal efficiencies and residual concentration on the 7th day of biofilm harvest. The asterisk (*) denotes a statistically significant ($p < 0.05$) difference in the removal efficiencies as determined by the *t*-test.

by fungus *Aureobasidium* sp. *MSP8* in 5 days, when grown under agitated (140 rpm) conditions (Zeng et al., 2021). This is comparable to the maximum phosphorous removal reported here (Fig. 3e), even though no agitation was used in the present study. Moreover, Zeng et al. reported that ~28% of the phosphorus was stored in EPS and around 45% of the uptake phosphorus was stored in the cells of the fungus. This is likely to be the case in the present study as increase in the phosphorus increased the EPS concentration (Fig. 1b).

3.4. Nitrification and denitrification

N. discreta biofilms were also found to be involved in nitrification and heterotrophic denitrification processes (Fig. 4). The highest ammonium removal efficiency observed was ~96% in the nitrogen trial (at the initial NH_4–N concentration of 0.022 g L^{-1}, total nitrogen = 0.044 g L^{-1}) (Fig. 4a). As the nitrogen concentration increased, there was a significant ($p < 0.05$) drop in the NH_4–N removal efficiency. The NH_4–N removal efficiencies were also found to decrease with increasing phosphorous concentration (Fig. 4b) but increased with increasing carbon concentration up to a carbon concentration of 4.21 g L^{-1}, beyond which it decreased once again (Fig. 4c).

Overall, high NO_3–N removal (denitrification) efficiencies were observed with 100% removal at the lower nitrogen concentrations (up to 0.175 g L^{-1}) (Fig. 4d) and greater than 90% removal at all phosphorous concentrations tested (Fig. 4e). In the carbon trial, low carbon concentrations affected NH_4–N and NO_3–N removal efficiencies significantly ($p < 0.05$) (Fig. 4c and f), which could be attributed to the trends seen in biofilm growth.

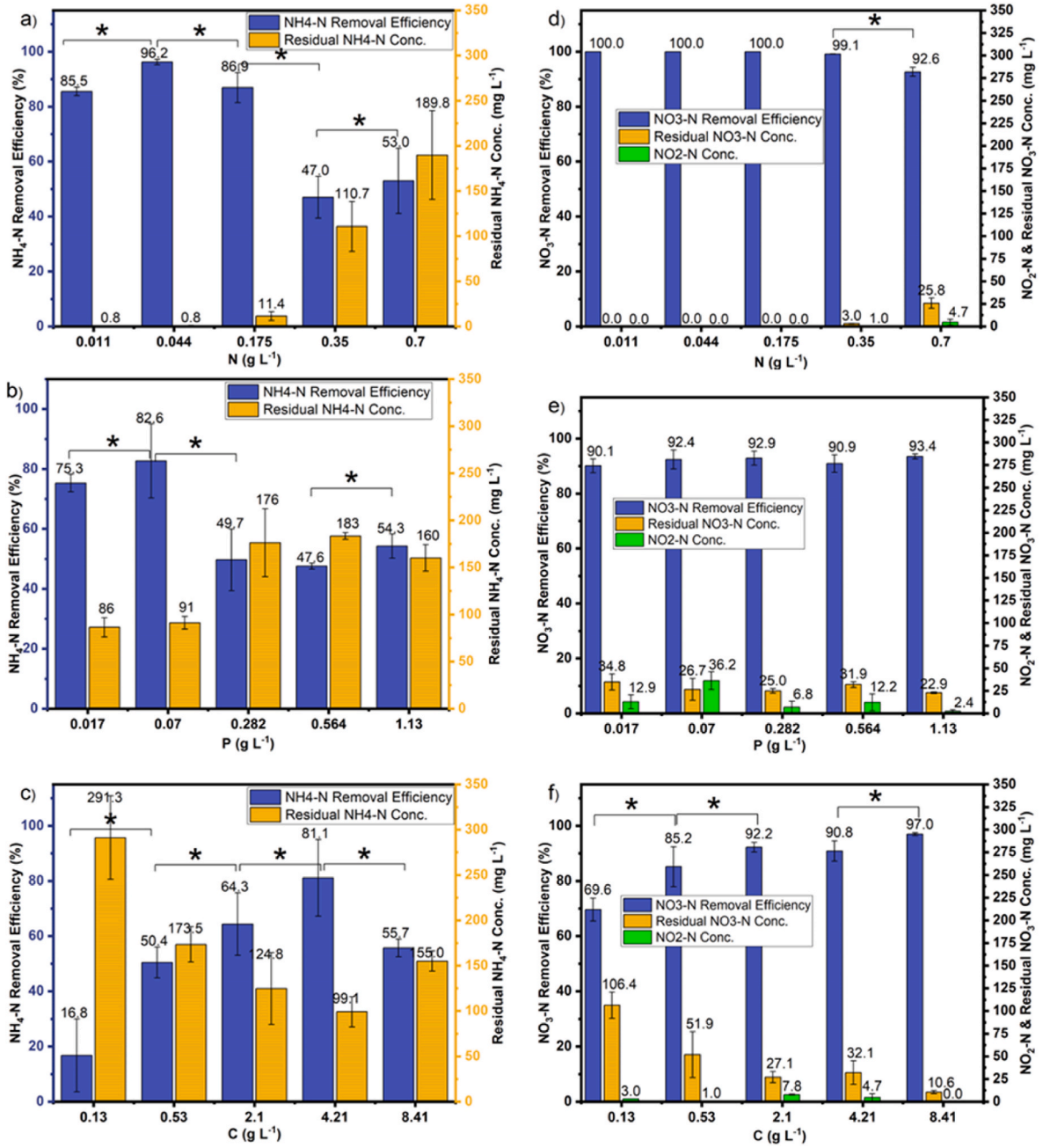

Fig. 4. Ammonium (a, b & c) and nitrate (d, e & f) removal efficiencies and residual nutrient concentrations at harvest. The asterisk (*) indicates that the removal efficiency difference in two conditions is statistically significant with $p < 0.05$ as determined by the *t*-test.

3.5. Nutrient removal rates and specific removal rates

In the nitrogen trial, NH_4–N, NO_3–N and carbon removal rates (mg L^{-1} d^{-1}) increased with increasing nitrogen concentration; however, phosphorus removal rates were lower at higher nitrogen concentrations (Fig. 5a). Specific removal rates (mg g^{-1} d^{-1}) of carbon and phosphorus were higher at lower nitrogen concentrations (Fig. 5b). In the phosphorus trial, the low phosphorus reactor biofilms promoted NH_4–N removal rates and specific removal rates (Fig. 5c and d) which led to the higher NH_4–N removal efficiency as well (Fig. 4b). The highest ammonium removal rates in the low phosphorus reactors (0.017 and 0.07 g L^{-1}) were around 37 mg L^{-1} d^{-1} (Fig. 5b) which is comparable to the nitrification rates of approximately 43 mg L^{-1} d^{-1} of a fungal strain of *Penicillium tropicum* in a batch reactor with planktonic growth (Yao et al., 2020).

Although nutrient removal rates in all cases were lower at low carbon levels (Fig. 5e), increased specific removal rates of NH_4–N, NO_3–N and phosphorus were observed as the carbon concentration was lowered from 8.41 to 0.13 g L^{-1} (Fig. 5f). As oxygen availability is an important factor in nitrification of NH_4–N, the lower oxygen requirements for carbon oxidation at lower carbon concentration reactors possibly resulted in higher specific nitrification rates (Fig. 5f). This is further confirmed by the higher concentration of DO in lower carbon reactors as seen from the supplementary data (Table S1).

The highest total nitrogen removal rate; including NH_4–N and NO_3–N removal rates was 82.9 mg L^{-1} d^{-1} (Fig. 5 c), which is nearly double the total nitrogen removal rates reported for *Penicillium tropicum* (43 mg L^{-1} d^{-1}) (Yao et al., 2020). A fungal strain of *Hanseniaspora uvariam* has been reported with NH_4–N and NO_3–N, and total nitrogen removal rates of ~30, 48, and 78 mg L^{-1} d^{-1}, respectively under agitated conditions (Zhang et al., 2018). The removal rates in the present study are therefore comparable or higher than those reported in the literature, despite being conducted with no agitation. These results demonstrate that *N. discreta* biofilms are a novel and promising alternative to bacterial HNADMs. A biofilm-based process would also have additional advantages over suspended cultures including easier separation of cells from the wastewater.

3.6. Correlations between nutrient removal rates and biofilm properties

It is important to evaluate the effects of nutrient concentrations in the wastewater on nutrient removal rates in conjunction with their effects on biofilm properties, as these parameters are closely interlinked. This section presents an integrated view of these effects supported by a heat map of Pearson's correlations between biofilm properties and nutrient removal rates (Fig. 6a–c) and proposes a pathway for the aerobic metabolism of nitrogen and phosphorous by *N. discreta* biofilms (Fig. 6d) based on these results.

As discussed in section 3.5, the specific rates of nutrient removal tended to be higher at low nutrient concentrations in the wastewater. Deficiency of one nutrient can cause stress, resulting in the accumulation and storage of the excess nutrients (Mason-Jones et al., 2021). This can

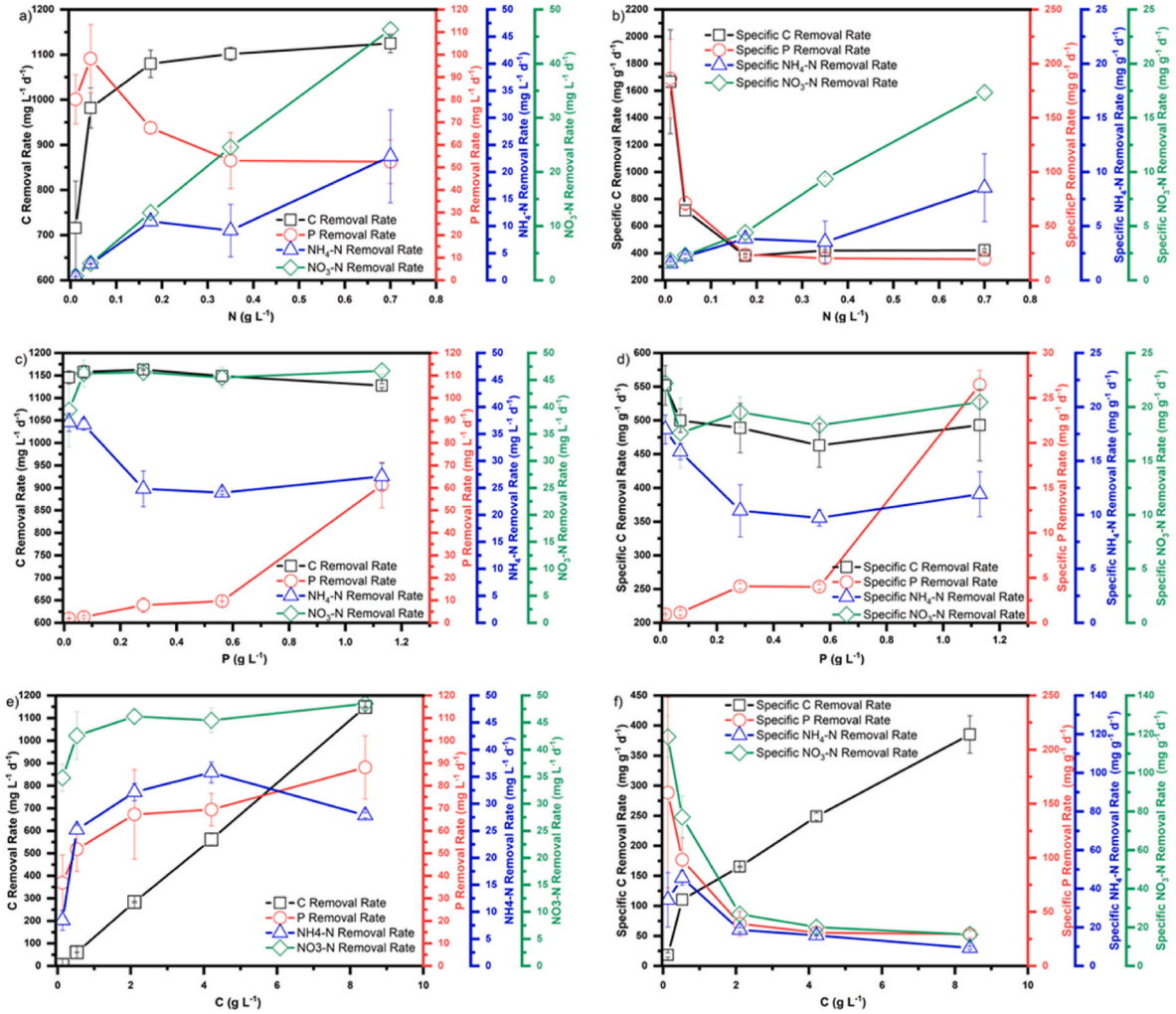

Fig. 5. Nutrient removal rates (mg L^{-1} d^{-1}) and specific removal rates (mg g^{-1} d^{-1}) of nitrogen trial (a, b), phosphorus trial (c & d) and carbon trial (e, f).

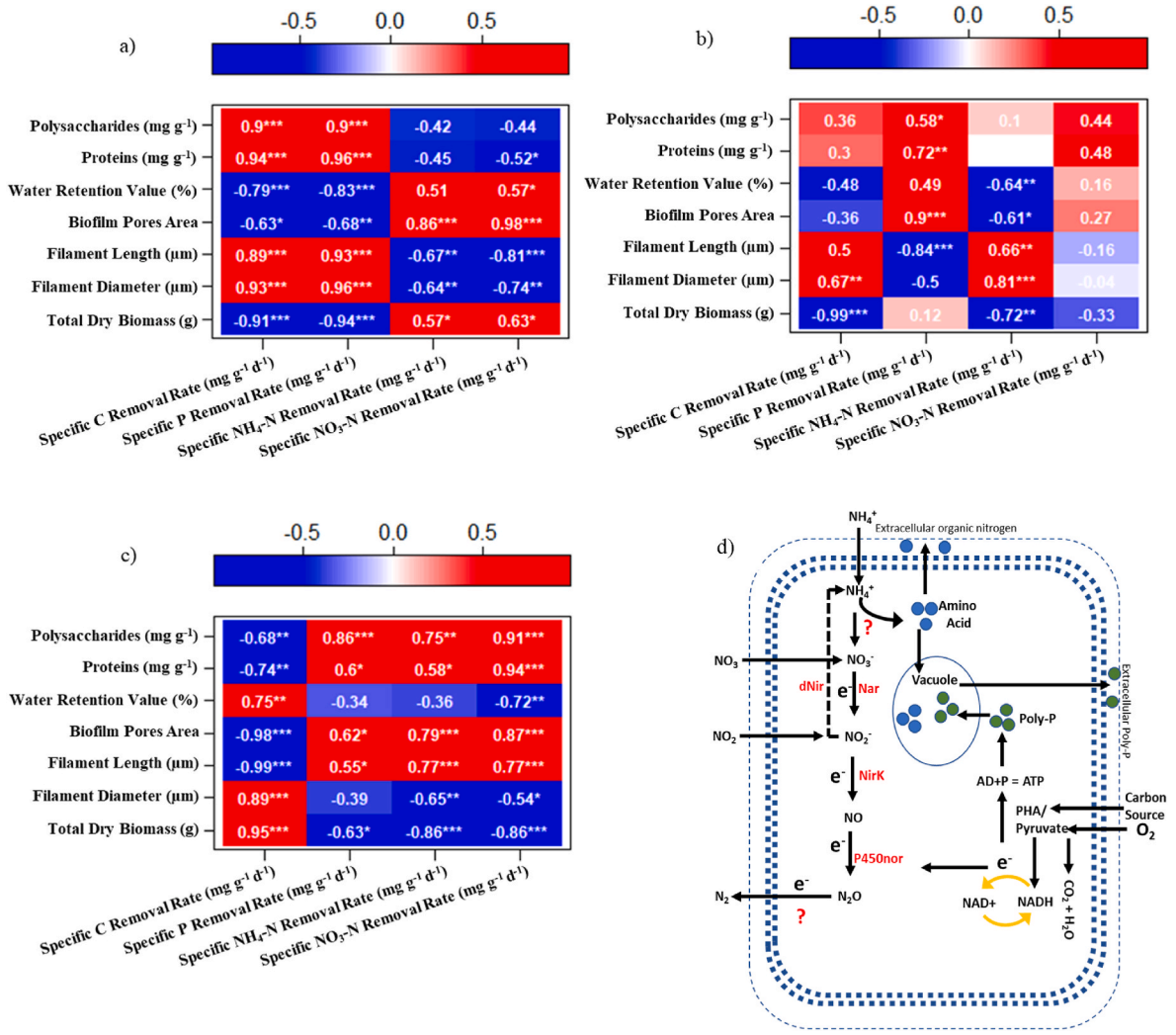

Fig. 6. Heat map of Pearson's correlations and proposed metabolic pathway. Correlations between nutrient removal and biofilm properties in (a) nitrogen, (b) phosphorus, and (c) carbon trial, "*": $p < 0.05$, "**": $p < 0.01$, "***": $p < 0.001$, "C": carbon, "P": phosphorus, (d) Proposed model for nitrogen and phosphorus aerobic metabolism of *Neurospora discreta*. "PHA": poly-β-hydroxyalkanoates, "Poly-P": polyphosphates, "NADH": nicotinamide adenine dinucleotide + hydrogen, NAD^+: oxidized form of NADH, "Nar": nitrate reductase, "NirK": nitrite reductase, "P450nor": cytochrome nitric oxide reductase.

be seen from the larger diameter of the filaments (Fig. 2a) and higher concentration of EPS (Fig. 1a) at low nitrogen concentrations as well as a significant positive correlation of the specific phosphate removal rate with filament length and diameter (0.93 and 0.96 respectively, $p <$ 0.0001) and with polysaccharide and protein concentrations (0.9 and 0.96 respectively, $p < 0.0001$) (Fig. 6a). This indicates that in this case, the energy required for denitrification was diverted to store the polyphosphate in the vacuole of the fungus and a large amount was secreted as EPS. EPS plays an important role in phosphate uptake and polyphosphates are secreted by cells through EPS (Li et al., 2015; Zhang et al., 2013). A part of the phosphorus is used for growth and the remaining is used for converting the adenosine diphosphate (ADP) to adenosine triphosphate (ATP) (Nehls and Plassard, 2018) which is stored in the vacuole. It can be inferred that in case of *N. discreta*, a relatively small quantity of phosphate was used for growth, as evidenced by the minimal effect of phosphorous on biofilm growth (Fig. 1b), with a larger proportion being accumulated inside the hyphae or stored in the EPS as seen from the correlations discussed above.

At lower phosphorous concentrations, the specific removal rate of carbon and NH_4–N increased significantly, and the fungus stored more PHA and amino acids, which increased the diameter of the fungus (Fig. 2b). Strong positive correlations between filament diameter and specific removal rate of carbon (0.67, $p < 0.001$) and NH_4–N (0.81, $p <$ *0.0001*) further support this argument (Fig. 6b). This is likely because the energy ($NADH \rightarrow NAD^+ + e^-$) required to store the higher concentration of phosphorus as poly-P was diverted for nitrification and denitrification in the biofilms of low phosphorus concentration reactors (higher C:P), as suggested in Fig. 6d.

From the carbon trial it was seen that low carbon concentrations resulted in lower filament diameters as seen from Fig. 2a. In this case, all the poly-β-hydroxyalkanoates (PHA) would have been consumed while investing in the storage of poly-phosphates (poly-P) and amino acids (Fig. 6d) (Mason-Jones et al., 2021). As carbon concentration increased, the utilization of carbon per unit biomass increased, resulting in lower porosity biofilms because of thicker filaments (Figs. 2c and 5e and f, 6c).

Although fungal nitrification-denitrification is not yet fully understood at the genetic level, a partial picture can be constructed based on the literature and results from the present study (Fig. 6d). A majority of the NH_4–N is assimilated into amino acids, and only a fraction of the NH_4–N is converted into nitrate (Zuo et al., 2021). Nitrate is reduced to nitrite by the nitrate reductase gene (Nar). The resulting nitrite is reduced to nitric oxide (NO) by nitrite reductase gene (NirK) followed by the production of nitrous oxide (N_2O) by cytochrome nitric oxide reductase (P450nor) (Aldossari and Ishii, 2021). The gene involved in N_2O conversion is unknown although it has been shown that up to 58% of the NO_3–N is converted into nitrogen gas (N_2) by some strains of cold

adapted fungi (Aldossari and Ishii, 2021).

In the present study, the denitrification efficiencies were significantly ($p < 0.05$) affected by carbon concentration (Fig. 4f). It is proposed that the energy required to activate the Nar/NirK/P450nor gene was not sufficient for complete denitrification at low carbon conditions. The NO_3–N removal rates were higher than NH_4–N removal rates which was the case in previously reported studies (Cheng et al., 2020; Yao et al., 2020), as denitrification (for NO_3–N removal) has a shorter metabolic pathway compared to nitrification-denitrification (for NH_4–N removal) (Fig. 6d).

Overall, these results demonstrate the ability of *N. discreta* biofilms for simultaneous and efficient removal of carbon, nitrogen, and phosphorous, and provide insight into the relationship between nutrient concentrations, biofilm properties and nutrient removal rates. In contrast with existing processes that require either multiple steps or the use of sequential batch reactors with alternating aerobic and anaerobic conditions (Nguyen Quoc et al., 2021; Regmi et al., 2022), this work can be used to design a single-step, aerobic process to treat wastewaters from a variety of sources, including high-strength industrial wastewaters containing high carbon and nitrogen content, such as those from the sugar, beverage, and fertilizer industries (Bhambri et al., 2021; Fuentes et al., 2021; Parande et al., 2009).

4. Conclusions

This work demonstrates simultaneous nitrification, aerobic denitrification, phosphorous uptake, and carbon removal from wastewater by *N. discreta* biofilms, indicating that it is a promising candidate for the biological treatment of carbon- and nitrogen-rich wastewater in a single aerobic reactor. The highest nitrification and denitrification rates were observed at a phosphorus concentration of 0.07 g L^{-1}, with ammonium and nitrate removal rates of 36.7 and 46.2 mg L^{-1} d^{-1}, respectively, and ammonium and nitrate removal efficiencies of 82.6 and 92.2%, respectively. The highest phosphorus removal rate of 98.2 mg L^{-1} d^{-1} with a removal efficiency of 60.9% was observed at a nitrogen concentration of 0.044 g L^{-1}. Carbon and nitrogen concentrations in the wastewater significantly affected the growth of the biofilms, whilst phosphorous concentration had no significant effect. The specific nutrient removal rates correlated well with biofilm properties including microstructure and EPS composition, indicating metabolic changes due to varying nutrient conditions.

CRediT author statement

Shamas Tabraiz: Conceptualization, Methodology, Investigation, Formal analysis, Writing – original draft. Aiswarya N M: Investigation. Himani Taneja: Investigation. R Aravinda Narayanan: Writing - Review & editing. Asma Ahmed: Writing - Review & editing, Supervision, Funding acquisition.

Declaration of competing interest

The authors declare that they have no known competing financial interests or personal relationships that could have appeared to influence the work reported in this paper.

Data availability

Data will be made available on request.

Acknowledgement

This work was supported by a Leverhulme Trust Research Project Grant (grant number: RPG-2020-021).

Appendix A. Supplementary data

Supplementary data to this article can be found online at https://doi.org/10.1016/j.jenvman.2022.116363.

References

Abràmoff, M.D., Magalhães, P.J., Ram, S.J., 2004. Image processing with imageJ. Biophot. Int. https://doi.org/10.1201/9781420005615.ax4.
Ahmed, A., Narayanan, R.A., Veni, A.R., 2020. Influence of carbon source complexity on porosity, water retention and extracellular matrix composition of Neurospora discreta biofilms. J. Appl. Microbiol. 128, 1099–1108. https://doi.org/10.1111/jam.14539.
Aldossari, Nouf, Ishii, S., 2021. Fungal denitrification revisited - recent advancements and future opportunities. Soil Biol. Biochem. https://doi.org/10.1016/j.soilbio.2021.108250.
Aldossari, N., Ishii, S., 2021. Isolation of cold-adapted nitrate-reducing fungi that have potential to increase nitrate removal in woodchip bioreactors. J. Appl. Microbiol. https://doi.org/10.1111/jam.14939.
Bhambri, A., Karn, S.K., Singh, R.K., 2021. In-situ remediation of nitrogen and phosphorus of beverage industry by potential strains Bacillus sp. (BK1) and Aspergillus sp. (BK2). Sci. Rep. https://doi.org/10.1038/s41598-021-91539-y.
Cao, F., Bourven, I., Guibaud, G., Rene, E.R., Lens, P.N.L., Pechaud, Y., van Hullebusch, E.D., 2018. Alteration of the characteristics of extracellular polymeric substances (EPS) extracted from the fungus Phanerochaete chrysosporium when exposed to sub-toxic concentrations of nickel (II). Int. Biodeterior. Biodegrad. https://doi.org/10.1016/j.ibiod.2018.02.009.
Cheng, H.Y., Xu, A.A., Kumar Awasthi, M., Kong, D.D., Chen, J.S., Wang, Y.F., Xu, P., 2020. Aerobic denitrification performance and nitrate removal pathway analysis of a novel fungus Fusarium solani RADF-77. Bioresour. Technol. 295 https://doi.org/10.1016/j.biortech.2019.122250.
Flemming, H.C., Wingender, J., 2010. The biofilm matrix. Nat. Rev. Microbiol. https://doi.org/10.1038/nrmicro2415.
Fuentes, K.L., Torres-Lozada, P., Chaparro, T.R., 2021. Beverage Wastewater Treatment by Anaerobic Digestion in Two-Stages for Organic Matter Removal and Energy Production. Biomass and Bioenergy. https://doi.org/10.1016/j.biombioe.2021.106260.
Ge, H., Batstone, D.J., Keller, J., 2015. Biological phosphorus removal from abattoir wastewater at very short sludge ages mediated bynovel PAO clade Comamonadaceae. Water Res. https://doi.org/10.1016/j.watres.2014.11.026.
Gonalves, C., Rodriguez-Jasso, R.M., Gomes, N., Teixeira, J.A., Belo, I., 2010. Adaptation of dinitrosalicylic acid method to microtiter plates. Anal. Methods. https://doi.org/10.1039/c0ay00525h.
He, Q., Rajendran, A., Gan, J., Lin, H., Felt, C.A., Hu, B., 2019. Phosphorus recovery from dairy manure wastewater by fungal biomass treatment. Water Environ. J. https://doi.org/10.1111/wej.12421.
Huang, F., Pan, L., He, Z., Zhang, Mengyu, Zhang, Mingzhu, 2020. Culturable heterotrophic nitrification-aerobic denitrification bacterial consortia with cooperative interactions for removing ammonia and nitrite nitrogen in mariculture effluents. Aquaculture 523, 735211. https://doi.org/10.1016/j.aquaculture.2020.735211.
Huang, F., Pan, L., Lv, N., Tang, X., 2017. Characterization of novel Bacillus strain N31 from mariculture water capable of halophilic heterotrophic nitrification–aerobic denitrification. J. Biosci. Bioeng. https://doi.org/10.1016/j.jbiosc.2017.06.008.
Huang, L.K., Wang, M.J.J., 1995. Image thresholding by minimizing the measures of fuzziness. Pattern Recognit. https://doi.org/10.1016/0031-3203(94)E0043-K.
Ji, J., Peng, Y., Wang, B., Li, X., Zhang, Q., 2020. A novel SNPR process for advanced nitrogen and phosphorus removal from mainstream wastewater based on anammox, endogenous partial-denitrification and denitrifying dephosphatation. Water Res. https://doi.org/10.1016/j.watres.2019.115363.
Li, W.W., Zhang, H.L., Sheng, G.P., Yu, H.Q., 2015. Roles of extracellular polymeric substances in enhanced biological phosphorus removal process. Water Res. https://doi.org/10.1016/j.watres.2015.06.034.
Liu, H., Fang, H.H.P., 2002. Extraction of extracellular polymeric substances (EPS) of sludges. J. Biotechnol. 95, 249–256. https://doi.org/10.1016/S0168-1656(02)00025-1.
Mason-Jones, K., Robinson, S.L., Veen, G.F., Ciska, Manzoni, S., van der Putten, W.H., 2021. Microbial storage and its implications for soil ecology. ISME J. https://doi.org/10.1038/s41396-021-01110-w.
Moore, D., Robson, G.D., Trinci, A.P.J., 2020. 21st Century Guidebook to Fungi, 21st Century Guidebook to Fungi. https://doi.org/10.1017/9781108776387.
Myszka, K., Czaczyk, K., 2009. Characterization of adhesive exopolysaccharide (EPS) produced by Pseudomonas aeruginosa under starvation conditions. Curr. Microbiol. https://doi.org/10.1007/s00284-009-9365-3.
Narayanan, R., Ahmed, A., 2019. Arrested fungal biofilms as low-modulus structural biocomposites: water holds the key. Eur. Phys. J. E 42. https://doi.org/10.1140/epje/i2019-11899-2.
Nehls, U., Plassard, C., 2018. Nitrogen and phosphate metabolism in ectomycorrhizas. New Phytol. https://doi.org/10.1111/nph.15257.
Nguyen Quoc, B., Armenta, M., Carter, J.A., Bucher, R., Sukapanpotharam, P., Bryson, S. J., Stahl, D.A., Stensel, H.D., Winkler, M.K.H., 2021. An investigation into the optimal granular sludge size for simultaneous nitrogen and phosphate removal. Water Res. https://doi.org/10.1016/j.watres.2021.117119.

Nielsen, P.H., McIlroy, S.J., Albertsen, M., Nierychlo, M., 2019. Re-evaluating the microbiology of the enhanced biological phosphorus removal process. Curr. Opin. Biotechnol. https://doi.org/10.1016/j.copbio.2019.03.008.

Pamidipati, S., Ahmed, A., 2017. Bio-processing of agricultural residues to bio-fuels using Neurospora discreta. 15th Int. Conf. Environ. Sci. Technol. 1–4.

Pamidipati, S., Ahmed, A., 2017. Degradation of lignin in agricultural residues by locally isolated fungus Neurospora discreta. Appl. Biochem. Biotechnol. https://doi.org/10.1007/s12010-016-2302-6.

Parande, A.K., Sivashanmugam, A., Beulah, H., Palaniswamy, N., 2009. Performance evaluation of low cost adsorbents in reduction of COD in sugar industrial effluent. J. Hazard Mater. https://doi.org/10.1016/j.jhazmat.2009.02.098.

Pathak, N, et al., 2020. Simultaneous nitrification-denitrification using baffled osmotic membrane bioreactor-microfiltration hybrid system at different oxic-anoxic conditions for wastewater treatment. J. Environ. Manag. 253.

Rashid, S.S., Liu, Y.Q., Zhang, C., 2020. Upgrading a large and centralised municipal wastewater treatment plant with sequencing batch reactor technology for integrated nutrient removal and phosphorus recovery: environmental and economic life cycle performance. Sci. Total Environ. https://doi.org/10.1016/j.scitotenv.2020.141465.

Regmi, P., Sturm, B., Hiripitiyage, D., Keller, N., Murthy, S., Jimenez, J., 2022. Combining continuous flow aerobic granulation using an external selector and carbon-efficient nutrient removal with AvN control in a full-scale simultaneous nitrification-denitrification process. Water Res. https://doi.org/10.1016/j.watres.2021.117991.

Ren, Y., Hao Ngo, H., Guo, W., Wang, D., Peng, L., Ni, B.J., Wei, W., Liu, Y., 2020. New perspectives on microbial communities and biological nitrogen removal processes in wastewater treatment systems. Bioresour. Technol. https://doi.org/10.1016/j.biortech.2019.122491.

Rey-Martínez, N., Badia-Fabregat, M., Guisasola, A., Baeza, J.A., 2019. Glutamate as sole carbon source for enhanced biological phosphorus removal. Sci. Total Environ. https://doi.org/10.1016/j.scitotenv.2018.12.064.

Romero-Olivares, A.L., Taylor, J.W., Treseder, K.K., 2015. Neurospora discreta as a model to assess adaptation of soil fungi to warming. BMC Evol. Biol. 15, 1–8. https://doi.org/10.1186/s12862-015-0482-2.

Sinha, E., Michalak, A.M., Balaji, V., 2017. Eutrophication will increase during the 21st century as a result of precipitation changes. Science 80. https://doi.org/10.1126/science.aan2409.

Song, T., Zhang, X., Li, J., Wu, X., Feng, H., Dong, W., 2021. A review of research progress of heterotrophic nitrification and aerobic denitrification microorganisms (HNADMs). Sci. Total Environ. https://doi.org/10.1016/j.scitotenv.2021.149319.

Sun, Z., Lv, Y., Liu, Y., Ren, R., 2016. Removal of nitrogen by heterotrophic nitrification-aerobic denitrification of a novel metal resistant bacterium Cupriavidus sp. S1. Bioresour. Technol. https://doi.org/10.1016/j.biortech.2016.07.110.

Tabraiz, S., Hassan, S., Abbas, A., Nasreen, S., Zeeshan, M., Fida, S., Shamurad, B.A., Acharya, K., Petropoulos, E., 2018. Effect of effluent and sludge recirculation ratios on integrated fixed films a2o system nutrients removal efficiency treating sewage. Desalination Water Treat. https://doi.org/10.5004/dwt.2018.22356.

Tang, Y., Zhang, M., Sun, G., Pan, G., 2019. Impact of eutrophication on arsenic cycling in freshwaters. Water Res. https://doi.org/10.1016/j.watres.2018.11.046.

Van Acker, Heleen, 2014. Molecular mechanisms of persistence in Burkholderia cenocepacia biofilms. https://biblio.ugent.be/publication/4412032.

Vogel, H. J, 1956. A convenient growth medium for *Neurospora crassa*. Microb. Genet. Bull. 13, 42–47.

Wang, Q., He, J., 2020. Complete Nitrogen Removal via Simultaneous Nitrification and Denitrification by a Novel Phosphate Accumulating Thauera Sp. Strain SND5. Water Res. https://doi.org/10.1016/j.watres.2020.116300.

Winkler, M.K., Straka, L., 2019. New directions in biological nitrogen removal and recovery from wastewater. Curr. Opin. Biotechnol. https://doi.org/10.1016/j.copbio.2018.12.007.

Wurtsbaugh, W.A., Paerl, H.W., Dodds, W.K., 2019. Nutrients, eutrophication and harmful algal blooms along the freshwater to marine continuum. WIREs Water. https://doi.org/10.1002/wat2.1373.

Yao, Z., Yang, L., Wang, F., Tian, L., Song, N., Jiang, H., 2020. Enhanced nitrate removal from surface water in a denitrifying woodchip bioreactor with a heterotrophic nitrifying and aerobic denitrifying fungus. Bioresour. Technol. https://doi.org/10.1016/j.biortech.2020.122948.

Zeng, X., Huang, J.J., Hua, B., 2021. Efficient phosphorus removal by a novel halotolerant fungus Aureobasidium sp. MSP8 and the application potential in saline industrial wastewater treatment. Bioresour. Technol. https://doi.org/10.1016/j.biortech.2021.125237.

Zhang, H., Zhao, Z., Kang, P., Wang, Y., Feng, J., Jia, J., Zhang, Z., 2018. Biological nitrogen removal and metabolic characteristics of a novel aerobic denitrifying fungus Hanseniaspora uvarum strain KPL108. Bioresour. Technol. 267, 569–577. https://doi.org/10.1016/j.biortech.2018.07.073.

Zhang, H.L., Fang, W., Wang, Y.P., Sheng, G.P., Zeng, R.J., Li, W.W., Yu, H.Q., 2013. Phosphorus removal in an enhanced biological phosphorus removal process: roles of extracellular polymeric substances. Environ. Sci. Technol. https://doi.org/10.1021/es403227p.

Zhang, J., Wang, C., Jiang, X., Song, Z., Xie, Z., 2020. Effects of human-induced eutrophication on macroinvertebrate spatiotemporal dynamics in Lake Dianchi, a large shallow plateau lake in China. Environ. Sci. Pollut. Res. https://doi.org/10.1007/s11356-020-07773-w.

Zhang, W., Seminara, A., Suaris, M., Brenner, M.P., Weitz, D.A., Angelini, T.E., 2014. Nutrient depletion in Bacillus subtilis biofilms triggers matrix production. New J. Phys. https://doi.org/10.1088/1367-2630/16/1/015028.

Zhao, J., Yuan, Q., Sun, Y., Zhang, J., Zhang, D., Bian, R., 2021. Effect of fluoxetine on enhanced biological phosphorus removal using a sequencing batch reactor. Bioresour. Technol. https://doi.org/10.1016/j.biortech.2020.124396.

Zuo, X., Xu, W., Wei, S., Grossart, H.P., Gao, Y., Luo, Z., 2021. Characterization of a novel aciduric and halotolerant aerobic denitrifying fungus Fusarium solani DS3 isolated from coastal seawater. Bioresour. Technol. Reports 16, 100839. https://doi.org/10.1016/j.biteb.2021.100839.